Measurement and Characterization of Indoor Ultra-Wideband Propagation

A. H. Muqaibel*, *Student Member, IEEE*, A. Safaai-Jazi*, *Senior Member, IEEE*, A. M. Attiya*, *Member, IEEE*, A. Bayram*, *Student Member, IEEE*, and S. M. Riad*, *Fellow, IEEE*

***Abstract*—The propagation of ultra-wideband (UWB) signals in indoor environments is an important issue with significant impacts on the future direction and scope of the UWB technology and its applications. The objective of this article is to present an assessment of the potentials of UWB indoor communications by characterizing UWB indoor channels. The channel characterization refers to extracting the channel parameters from measured propagation data. An indoor UWB measurement campaign is undertaken. Time-domain indoor propagation measurements using pulses with FWHM equal to 85 ps are carried out. Typical indoor scenarios, including line-of-sight (LOS), non-line-of-sight (NLOS), room-to-room, within-the-room, and hallways are considered. Results of indoor propagation measurements are presented for local power delay profiles (local PDP) and small-scale averaged power delay profiles (SSA-PDP). Site-specific trends and general observations are discussed. The results for path-loss exponent and time dispersion parameters are presented.**

***Index Terms*:** UWB Indoor Propagation, UWB Communications

I. Introduction

Ultra wideband (UWB) wireless communication has been the subject of extensive research in recent years due to its potential applications and unique capabilities. However, many important aspects of UWB-based communication systems have not yet been thoroughly examined. The propagation of UWB signals in indoor environments is one of the important issues with significant impacts on the future direction, scope, and generally the extent of the success of UWB technology. Researchers are nowadays devoting considerable efforts and resources to develop robust channel models that allow for reliable and accurate ultra-wideband performance simulation.

In the past two decades, significant research work has been devoted to narrowband indoor channel characterization. Of particular interest are investigations carried out by Saleh and Valenzuela [1], Hashemi [2], Anderson *et al.* [3] and Durgin and Rappaport [4], whose primary objectives have been to develop channel models that describe the system performance adequately. Successful channel characterizations require extensive and accurate propagation measurements. At present, the amount of available UWB measurement data is very limited and more information is needed to support a comprehensive channel modeling study. The issue becomes more complicated due to the fact that UWB pulse measurements are antenna dependent. The spectrum and the shape of the pulse also affect the measurement results.

The analysis of indoor communication systems based on simulation of the entire transmission link using statistical methods is most useful in assessing the system performance [2]. This approach, however, requires extensive propagation measurements. Some research work on both deterministic [5] and statistical modeling [6] has been reported. More recently, Cassioli et al. [7] presented simulation results for UWB indoor communications, while Chalillou *et al.* [8] discussed the main structure of a general simulator for UWB communication systems. However, there still remain many unresolved issues and hence the need for more UWB propagation measurements. Different measurement conditions, insufficient measurement data, and the effect of different excitation pulses are among the issues that justify additional measurements in order to develop robust models for UWB indoor channels.

Recently, Scholtz, and Win conducted a UWB time-domain measurement campaign [9]. The results of their measurements were later used to develop further models [7], [10], but no information on the pulse shape and the characteristics of the antennas used in their measurements are explicitly provided. Only in a separate study it is mentioned that a diamond-shape dipole antenna has been used [11]. In order to achieve a more realistic characterization of UWB channels, Withington *et al.* [12], and Dickson and Jett [13] used modulated and time dithered pulses to emulate real communication environments. However, if the transfer function or the impulse response of the channel is known, it will be a relatively straightforward task to study the effects of time dithering or any other techniques through simulation.

The objective of this paper is to present time-domain measurements and characterization of ultra-wideband (UWB) propagation in indoor environments and to detail the experimental procedures and measurement setup used to collect data. First, experimental procedures and locations where the measurements were carried out are described. Then, post processing of the acquired data is explained. Finally, the results pertaining to small-scale effects, large-scale path-loss exponents, and time dispersion parameters are discussed. Some site-specific trends and observations are described and channel performances for two types of directive and omni-directional antennas are compared.

* Time-Domain and RF Measurement Laboratory, Bradley Department of Electrical and Computer Engineering, Virginia Polytechnic Institute and State University, Blacksburg, VA 24061-0111; email: ajazi@vt.edu. This work was supported in part by the Defense Advanced Research Projects Agency.

0-7803-8187-4/03/$17.00 ©2003 IEEE

II. Measurement Procedure and Locations

Time-domain measurements were performed using a sampling oscilloscope as receiver and a Gaussian-like pulse generator as transmitter. Two low noise wideband amplifiers were used at the receiver side. Each amplifier has a again of 10 dB and a 3dB-bandwidth of 15 GHz. The full-width half-maximum (FWHM) of the excitation pulse is 85 ps. Offset calibration is carried out with a matched load before performing any measurements. The received signals were sampled at a rate of 1 sample per 10 ps. An acquisition time window of 100 ns was selected to ensure that all observable multipath components are accounted for. This time window is consistent with the maximum excess delay of 70 ns reported by other investigators [14]. The sampling oscilloscope allows a maximum of 5K points at a time. The 5K points correspond to 50 ns time window. Two measured 50 ns time windows were cascaded to yield a 100 ns acquisition time. A total of about 400 profiles were collected. The spatial width of the pulse used in our measurements is much smaller than those used in previously published measurements. The spatial width is small enough to make the line-of-sight path always resolvable from any other multipath component.

In indoor environments, the time-varying part of the impulse response is typically due to human movements. By conducting measurements during low activity periods and by keeping both the transmitter and the receiver stationary, the channel can be treated as being quasi-stationary. This allows us to average 32 measurements, thus effectively canceling out the noise.

Two different sets of measurements were performed using highly directional TEM horn antennas and omni-directional biconical antennas. Both transmit and receive antennas were placed on plastic carts at an elevation of about 1.25 m above the floor. Styrofoam slabs were used to adjust the elevation without introducing significant reflections around the antennas. The TEM horn antennas were aligned for maximum boresight reception. With TEM horns, fewer multipath components are received and almost none from rear directions of the receiver. Biconical antennas are omni-directional and are a better representative of antennas for use in mobile UWB applications. The biconical antennas used in this investigation have not been designed as impulse antennas but have very wide input-impedance bandwidth.

Two levels of measurements are performed to characterize the small-scale and the large-scale fading parameters of the channel. Initially, a 7×7 grid with 15 cm spacing between adjacent points was designed and used in the measurements. However, after observing that no small-scale fading due to phase cancellation occurs, only a 3×3 measurement grid with 45 cm spacing between adjacent points was used. The triggering signal was carried by a coaxial cable to the sampling oscilloscope. It was noted that as the distance between transmitter and receiver increases the loss and dispersion in the triggering cable increase too, resulting in a higher jitter. An effort was made to use higher quality cables and minimum possible lengths for the trigger signal. A personal computer was used to store and post process the data.

The measurements were carried out in two buildings on Virginia Tech campus; namely, in Whittemore Hall and in Durham Hall. The first building is mainly comprised of offices and classrooms with most walls made of drywalls and metallic studs. Some walls at certain locations including stairwells are made of cinderblock and poured concrete. In Durham Hall, the interior walls are largely made of drywalls and cinderblocks. The floor is covered with tiles in hallways and with carpet inside the rooms. An advantage of performing UWB experiments in these buildings is that they have been characterized for some narrowband frequency ranges and site-specific ray tracing studies [3], [15], [16]. This allows one to compare the narrowband and the UWB channel characterization results.

III. Signal Processing and Data Analysis

A major challenge in UWB channel measurements is that the measurement bandwidth is open to many radiated signals. When taking measurements close to utility rooms or laboratories, where electromagnetic radiation level is high, there is an apparent increase in the noise floor. To reduce the interference from undesirable sources, the acquired signal profile is filtered in order to remove some signals that are not part of the transmitted pulse. The 3 dB bandwidth of the bandpass filter used for interference rejection occupies a frequency range from 0.1 GHz to 12 GHz. The corner frequencies of the filter are chosen by observing the spectrum of the radiated pulse and making sure that there is no significant energy outside the filter passband. It was noted that the pulse generator gives off low frequency components in the 30 MHz range that can be picked up by the biconical antenna.

Precursor and noise before the arrival of the first component are forced to zero in the processing stage. For energy calculations and large-scale path-loss analysis, a noise threshold is introduced below which all data are assumed to be zero. The threshold was set at 6 dB above the noise floor determined as the maximum level of the profile tail in the last 5 ns of the 100 ns time window.

A. Small-Scale Fading

In narrowband communication systems, small-scale fading describes signal drop due to destructive interference of the multipath components at the receiver when sub-wavelength changes are made in the receiver position [4], [22]. The concept of small-scale fading may be extended to UWB communications as the destructive interference of multipath components at the receiver due to a change in its position in the order of fraction of spatial width of the transmitted pulse.

Sample results are presented for measured delay profiles, referred to as local power delay profiles (local PDP) and for small-scale averaged power delay profiles (SSA-PDP). In SSA-PDPs, nine measurements are properly delayed and averaged. Figure 1 illustrates how SSA-PDPs are different from the local PDPs. The first three plots, Figure 1a to 1c, are

local PDPs and Figure 1d is the average of all 9 local measurements. When delay-and-average is used, the line-of-sight components tend to prevail and the other components spread out on the time axis such that they do not add coherently because of the high resolution of the transmitted pulse. Small-scale processing shows the capability for using a delay-and-sum beamformer to process a received array of signals from different antennas located in a very small area [18].

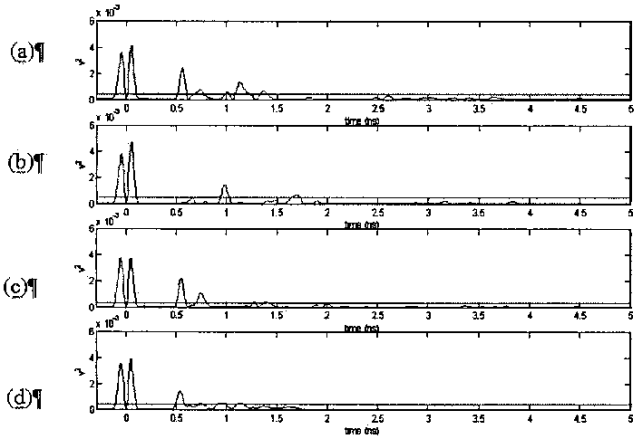

Fig. 1. Comparison between small-scale averaged power delay profiles and local power delay profiles. Measurements were performed with TEM horn antennas in Whittemore, 2nd floor. (a) Measured power delay profile (PDP) at location (1,1), (b) measured power delay profile (PDP) at location (1,4), (c) measured power delay profile (PDP) at location (1,7), (d) small-scale averaged power delay profiles (SSA-PDP) for the nine measurements on the grid.

B. Path Loss and Large-scale Analysis

The energy in the received profile decreases with the distance between the receiver and the transmitter. The path-loss exponent, n, is a measure of decay in signal power with distance, d, according to $1/d^n$. A reference measurement is performed at a distance of 1 m form the transmitter. Subsequent signal measurements are performed with respect to the reference measurement. Using the log-normal shadowing assumption, the path-loss exponent, n, is related to the received energy at distance d and the reference measurement by

$$PL(d) = \overline{PL}(d_0) + 10n\log_{10}(d/d_0) + X_\sigma \qquad (1)$$

where d_0 is the reference distance, $\overline{PL}(d_0)$ is the average measured energy at the reference distance and X_σ is a zero-mean Gaussian-distributed random variable in dB with standard deviation equal to σ [22]. The path-loss exponent is obtained by fitting a line on the logarithmic scatter plot of energy versus distance. The standard deviation for the Gaussian random variable is obtained by calculating the deviation from the obtained fit. The reference measurement is very important as it defines the intercept with the vertical axis and hence affects the fitted slope. Many reference measurements can be averaged together to reduce the effect of the measurement environment.

In narrowband characterization, the local PDPs and small-scale averaged PDPs (SSA-PDP) are usually used to eliminate any small-scale effect. The same technique is implemented by Cassioli *et al.* [7] to generate local and global parameters. In the present analysis, the UWB pulse delay time is used to find the distance between the receiver and the transmitter. First, the distance between the transmitter and the receiver is measured at a reference position. Then, other distances separating the receiver from the transmitter are calculated using the pulse delay time. This allows us to take measurements at locations with small separation distances and reduce the error associated with distance measurements. Measured points are distributed across the entire scatter plots rather than being clustered. This distribution reduces the error associated with reference measurements. The scatter plots for global data are presented in Figure 2.

TABLE I
LARGE-SCALE PATH-LOSS PARAMETERS FOR TEM HORN AND BICONICAL ANTENNAS

Antenna	TEM Horn		Biconical	
Location	n	σ	n	σ
W & D	1.8274	5.7291	1.7482	4.2585
W	1.5602	1.7196	1.5653	2.0095
W2	1.5454	1.6763	1.5807	1.3494
W4	1.2744	0.4763	1.3035	1.9032
W6	1.7845	0.7160	1.8192	1.0235
D	2.0401	6.5007	1.9103	4.8007
D1	3.2883	2.6456	2.9655	1.8769
D2	1.6591	1.0542	1.5365	1.5381
D3	1.7986	2.3358	1.7983	2.2394
D4	1.6478	1.3841	1.7870	3.9154
D5	2.6701	5.6894	2.2455	1.8009
LOS	1.6077	1.5816	1.5826	1.9135
NLOS	2.6039	6.0840	2.4118	3.2698

W: Whittemore Hall, D: Durham Hall

The extracted parameters for LOS and NLOS scenarios are summarized in Table 1. The minimum path-loss exponent is 1.27 for the case of a narrow corridor which has nearly the behavior of a lossy waveguide structure. The maximum pathloss exponent is 3.29 in some obstructed scenarios. The global line-of-sight parameters are n=1.61 and σ=1.58 dB for the TEM horns and n=1.58 and σ=1.91 dB for the biconical antennas. The NLOS scenarios have path-loss exponents greater than 2 and also have larger σ values compared with LOS scenarios.

In general, there is close agreement between the results obtained with directive antennas and the results obtained with omni-directional antennas. A notable difference is lower σ values when directive antennas are used for NLOS scenarios since any object in the channel can easily shadow directive antenna. However omni-directional antennas can still receive some components even in the case of NLOS.

The reported path-loss exponents for narrowband systems are 1.6-1.8 for indoor line-of-sight environments and 4-6 for obstructed indoor environments [22]. As noted from Table 1, the path-loss exponents for UWB are comparable with path-loss exponents for narrowband LOS scenarios but are smaller for NLOS scenarios. The results for path-loss exponent and the standard deviation introduced by Ghassemzadeh *et al.* [19] are comparable to the results obtained from our

measurements. They performed UWB frequency-domain measurements around 5 GHz [19], which is close to the center frequency in the spectrum of the pulse used in our experiments. Their parameters are n=1.7, σ=1.6 dB for LOS scenarios and n=3.5, σ=2.7 dB for NLOS scenarios.

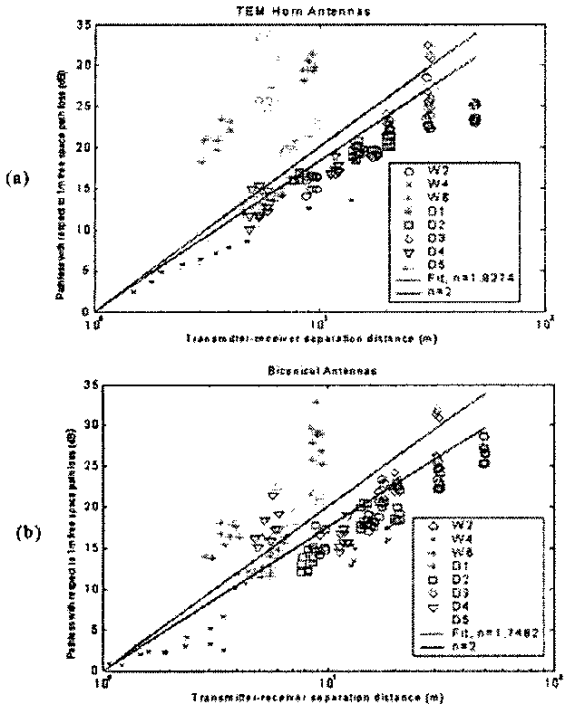

Fig. 2. Scatter plots for the relative path-loss versus distance for all locations (a) for TEM horn antennas, (b) for biconical antennas.

C. *Time Dispersion Results*

Time dispersion parameters shed some light on the temporal distribution of power relative to the first arriving components. Delay spreads restrict transmitted data rates and could limit the capacity of the system when multi-user systems are considered. The time dispersion of UWB pulses can be presented as the ratio of the average arrival time to the spread of the arrival time. The formulation of time dispersion parameters is given in [22].

The ratio of the mean excess delay to the RMS delay spread can be used as a measure of the time dispersion for UWB signals. If $\sigma_\tau = \bar{\tau}$, then the multipath delay profile decays exponentially. The situation corresponds to two multipath components with equal power where the second path is $2\bar{\tau}$ away from the first component. High concentration of power when the excess delay is small is reflected by $\bar{\tau}/\sigma_\tau$<1. When energy arrives at the mid point of the power delay profile and not at the earliest part then $\bar{\tau}/\sigma_\tau$>1 [21].

The cumulative distribution function (CDF) for the RMS delay spread is plotted in Figure 3. All multipath components within 20 dB of the maximum are included. It is observed that obstructed and non-line-of-sight scenarios result in higher time dispersion. The variations between different scenarios and buildings are less for the omnidirectional antennas than those when directive TEM horns are used. For the biconical antennas the values are higher because the receiving bicone antenna can receive more multipath components. It should be noted that the instantaneous delay spreads cannot be averaged to give the delay spread. Instead, for the SSA-PDPs, the power delay profiles are averaged and then the delay spread is calculated. Individual power delay profiles are averaged and weighted by their own power [20].

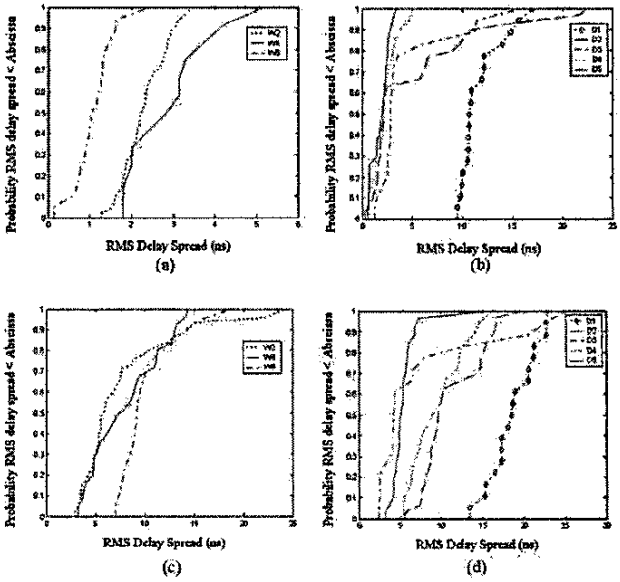

Fig. 3. Cumulative distribution functions for the RMS delay spread (20 dB) vs. RMS delay spread (ns): (a) Whittemore Hall using TEM horn antenna, (b) Durham Hall using TEM horn antenna, (c) Whittemore Hall using biconical antenna, (d) Durham Hall using biconical antenna.

Next, the correlation between the channel time dispersion parameters is examined. The relation between the mean excess delay and the RMS delay spread is illustrated in Figure 4. The ratio $\bar{\tau}/\sigma_\tau$ is mostly in the range of 0.25 to 1. The small values for this ratio imply high concentration of power at small excess delay. Obstructed measurements tend to have $\bar{\tau}/\sigma_\tau$=1 which means that the power decays exponentially with time. For the LOS scenarios the mean excess delay is close to zero, indicating that only the LOS component is within the specified level of power. The number of dominant multipath components is limited to two in LOS scenarios. This is consistent with the results of previous measurements carried out at the same locations in Durham Hall [17].

The scatter analysis of our UWB measured data indicates that there is no relationship between delay spread and transmitter-receiver separation. This is in agreement with that reported in [1] and [21] for narrowband systems. On the other hand, when considering the relation between the received energy and the delay spread, lower energy signals might seem to have larger excess delay. However, this is because the locations where the received energy is low are usually obstructed and signals arrive at the receiver through many

paths. In general, received power is not correlated to the excess delay parameters. Also, in [1] and [21] scatter plots of RMS delay spread versus path-loss indicate no correlation.

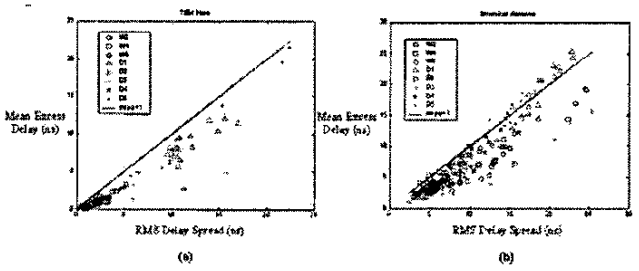

Fig. 4. Scatter plots for the mean excess delay (ns) versus the RMS delay spread (ns), (a) TEM horn antenna, (b) Biconical antenna

IV. CONCLUSIONS

Time-domain measurements were presented for ultra-wideband indoor channel characterization. The performed measurements have sufficiently high resolution necessary for development of accurate UWB communication channel models. The high-resolution pulses used in these measurements are good candidates for small cell scenarios, such as single-cell-per-room where few obstructions exist. Directive TEM horn and omni-directional biconical antennas were used in the measurements and their impacts on received signals were compared. Site-specific trends and general observations were also discussed. Some statistical analyses of the measured data were presented and compared with the previously published UWB and narrowband results. These measurements and the corresponding statistical analyses indicate that, unlike narrowband signals, UWB signals are immune to multipath fading. The calculated path-loss exponent was as low as 1.27 for a narrow corridor. For LOS and NLOS scenarios the global path-loss exponents were found to be nearly 1.6 and 2.7, respectively. The calculated time dispersion parameters for the measured results indicate high concentration of power at low excess time delays.

REFERENCES

[1] A. A. Saleh and R. A Valenzuela, "A Statistical Model for Indoor Multipath Propagation," *IEEE J. Selected Areas Commun.*, vol. 5, pp.128-137, 1987.

[2] H. Hashemi, "The Indoor Radio Propagation Channel," *Proc. IEEE*, vol. 81, no. 7, pp. 943 -968, 1993.

[3] C. R. Anderson, T. S. Rappaport, K. Bae, A. Verstak, N. Ramakrishnan, W. Tranter, C. Shaffer, and L. Watson, "In-Building Wideband Multipath Characteristics at 2.5 & 60 GHz," *Proceedings of IEEE 56th Vehicular Technology Conference*, vol.1, pp. 97-101, 2002.

[4] G. D. Durgin, and T. S. Rappaport, "Theory of Multipath Shape Factors for Small-Scale Fading Wireless Channels," *IEEE Transactions on Antennas and Propagation*, vol. 48, no. 5, pp. 682-693, 2000.

[5] B. Uguen, E. Plouhinec, and G. Ghassay, "A Deterministic Ultra Wideband Channel Modeling," *IEEE Conference on Ultra Wideband Systems and Technologies*, Proc. pp. 1-5, 2002.

[6] F. Zhu, Z. Wu, and C Nassar, "Generalized Fading Channel Model with Application to UWB," *IEEE Conference on Ultra Wideband Systems and Technologies*, Proc. pp. 13-17, 2002.

[7] D. Cassioli, M. Win, and A. Molisch, "The Ultra-Wide Bandwidth Indoor Channel: From Statistical Model to Simulations," IEEE Journal on Selected Areas in Communications, vol. 20, no. 6, pp. 1247-1257, 2002.

[8] S. Chalillou, D. Helal, and C Cattaneo, "Timed Simulator for UWB Communication Systems," *IEEE Conference on Ultra Wideband Systems and Technologies*, Proc. pp. 6-11, 2002.

[9] R. A. Scholtz and M. Z. Win, "Impulse Radio," *IEEE PIMRC'97-Helsinki, Finland.* Proc. pp. 245-267, 1997.

[10] R. Cramer, R. A. Scholtz and M. Z. Win, "Evaluation of an Ultra Wideband Propagation Channel," *IEEE Transactions on Antennas and Propagation*, vol. 50, no. 5, pp. 561-570, 2002.

[11] H. G. Schantz and L. Fullerton, " The Diamond Dipole: A Gaussian Impulse Antenna," *IEEE International Symposium Antenna and Propagation Society*, proc. vol. 4, pp. 100-103, 2001.

[12] P. Withington, R. Reinhardt, and R. Stanley, "Preliminary Results of an Ultra-Wideband (impulse) Scanning Receiver," *IEEE Conference Proceedings on Military Communications*, MILCOM'99, vol. 2 , pp. 1186 –1190, 1999.

[13] D. Dickson and P. Jett, "An Application Specific Integrated Circuit Implementation of a Multiple Correlator for UWB Radio Applications," *in IEEE Proc. Military Communications Conf.*, vol. 2, pp. 1207-1210, 1999.

[14] V. Hovinen, M. Hämäläinen, and T. Pätsi, "Ultra Wideband Indoor Radio Channel Models: Preliminary Results," *IEEE Conference on Ultra Wideband Systems and Technologies*, Proc. pp. 75-79, 2002.

[15] S. Sediel, and T. Rappaport, "Site-Specific Propagation Prediction for Wireless In-Building Personal Communication System Design," IEEE Transactions on Vehicular Technology, vol. 43, no. 4, pp. 879-891, 1994.

[16] D. A. Hawbaker, "Indoor Wideband Radio Wave Propagation Measurements and Models at 1.3 GHz and 4.0 GHz," M.S. Thesis, Dept. Elec. Eng., Virginia Polytech. Inst. And State Univ., 1991.

[17] C. R. Anderson, "Design and Implementation of an Ultrabroadband Millimeter-Wavelength Vector Sliding Correlator Channel Sounder and In-Building Multipath Measurements at 2.5 & 60 GHz", MS Thesis, Dept. Elect.& Comp. Eng., VPI & SU, 2002.

[18] R. J.-M. Cramer, M. Z. Win, and R. A. Scholtz, "Impulse radio multipath characteristics and diversity reception," *IEEE Int. Conf. on Comm.*, Conference Record, vol. 3, pp. 1650-1654, 1998.

[19] S. Ghassemzadeh, R. Jana, C. Rice, and W. Turin, "A Statistical Path Loss Model for In-Home UWB Channels," *IEEE Conference on Ultra Wideband Systems and Technologies*, Proc. pp. 59-64, 2002.

[20] R. G. Vaughan and N. Scott, "Super-Resolution of Pulsed Multipath Channels for Delay Spread Characterization," *IEEE Transactions on Communications*, vol. 47, no.3, pp. 343-347, 1999.

[21] T. S. Rappaport, "Characterization of UHF Multipath Radio Channels in Factory Buildings," *IEEE Transactions on Antennas and Propagation* , vol. 37, no. 8 , pp. 1058 –1069, 1989.

[22] T. S. Rappaport, *Wireless Communications, Principles & Practice*, Prentice Hall, Inc. 1996.